

## Stress Intensity Factor of an Interface Crack in a Bonded Plate under Uni-Axial Tension\*

Nao-Aki NODA\*\*, Yu ZHANG\*\*, Xin LAN\*\*, Yasushi TAKASE\*\*  
and Kazuhiro ODA\*\*\*

\*\* Department of Mechanical and Control Engineering, Kyushu Institute of Technology,  
1-1 Sensui-cho, Tobata-ku, Kitakyushu-shi, Fukuoka, Japan  
E-mail: noda@mech.kyutech.ac.jp

\*\*\* Tokuyama College of Technology, Gakuendai, Shunan-shi, Yamaguchi, Japan

### Abstract

Although a lot of interface crack problems were previously treated, few solutions are available under arbitrary material combination. This paper deals with a central interface crack in a bonded infinite plate and finite plate. Then, the effects of material combination on the stress intensity factors are discussed. A useful method to calculate the stress intensity factor of interface crack is presented with focusing on the stress at the crack tip calculated by the finite element method. For the central interface crack, it is found that the results of bonded infinite plate under remote uni-axial tension are always depending on the Dunders' parameters  $\alpha, \beta$  and different from the well-known solution of the central interface crack under internal pressure that is only depending on  $\beta$ . Besides, it is shown that the stress intensity factor of bonded infinite plate can be estimated from the stress of crack tip in the bonded plate when there is no crack. It is also found that dimensionless stress intensity factor  $F_I < 1$  when  $(\alpha + 2\beta)(\alpha - 2\beta) > 0$ ,  $F_I > 1$  when  $(\alpha + 2\beta)(\alpha - 2\beta) < 0$ , and  $F_I = 1$  when  $(\alpha + 2\beta)(\alpha - 2\beta) = 0$ .

**Key words:** Elasticity, Stress Intensity Factor, Fracture Mechanics, Finite Element Method, Interface Crack, Bonded Plate

### 1. Introduction

An interface crack in an infinite bonded plate under internal pressure in Fig.1 (a) is known as the most fundamental and well known solution for interface cracks. The stress intensity factor is given in Eq.1.

$$K_I + iK_{II} = (F_I + iF_{II})(1 + 2i\varepsilon)\sigma\sqrt{\pi a}, \quad F_I = 1, \quad F_{II} = 0 \quad (1)$$

It is also known that the interface crack under remote biaxial tension as shown in Fig.1 (b) is equivalent to the one in Fig.1 (a). In Fig.1 (b),  $\sigma_y^\infty = \sigma$  is the remote tensile stress in the y direction, and  $\sigma_{x1}^\infty, \sigma_{x2}^\infty$  are the ones in the x direction so as to produce the same strain in the x direction  $\varepsilon_{x1} = \varepsilon_{x2}$  along the bi-material interface<sup>(1)</sup>. As shown in Fig.2 (a), a central interface crack in a bonded plate has been treated in the previous studies<sup>(2)-(4)</sup>, and some noticeable results are provided in Table 1. As can be seen from this table, those results almost coincide with each other. However, the limiting solution as  $a/W \rightarrow 0$  in Table 1 has not been discussed yet in the previous studies. In Table 1 it is seen that dimensionless stress intensity factor  $F_I$  does not approach unity although  $F_{II} \rightarrow 0$  as  $a/W \rightarrow 0$ . In other words, it is confirmed that the solution under uni-axial tension in Fig.3 (b) is not equivalent to Eq. (1).

\*Received 16 Nov., 2009 (No. e84-1)  
[DOI: 10.1299/jmmp.4.974]

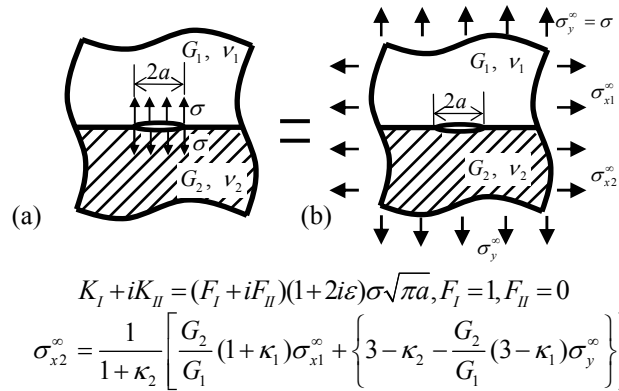


Fig.1 Infinite bonded plate subjected to (a) internal pressure and (b) remote biaxial tensile stress.

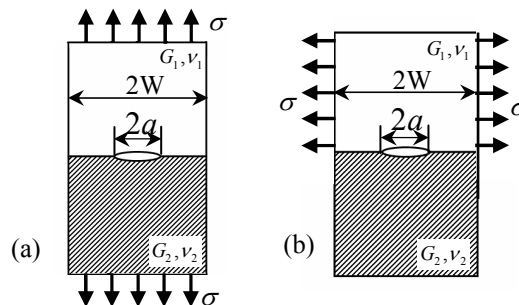


Fig.2 Bonded finite plate with a central interface crack .

Table 1 Dimensionless stress intensity factors of center interface crack in bonded plate (see Fig 2, Plane stress,  $\nu_1 = \nu_2 = 0.3$ ).

$\frac{G_2}{G_1}$	$a/W$	$F_I$			$F_{II}$		
		Ref. [2]	Ref. [3]	Ref. [4]	Ref. [2]	Ref. [3]	Ref. [4]
4	→0	?	?	?	?	?	?
	0.1	0.986	0.981	0.986	0.005	0.005	0.005
	0.2	1.005	1.005	1.005	0.009	0.010	0.009
100	→0	?	?	?	?	?	?
	0.1	0.943	0.941	0.943	0.008	0.008	0.009
	0.2	0.960	0.960	0.960	0.017	0.018	0.018

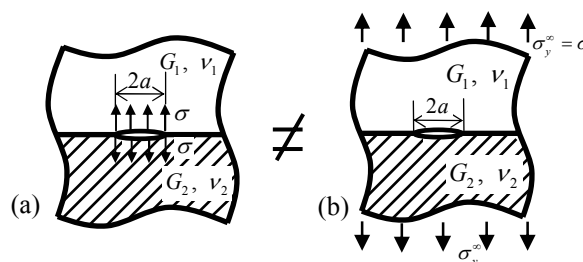


Fig.3 Infinite bonded plate subjected to (a) internal pressure and (b) remote uni-axial tensile stress.

In this study, stresses at the interface crack tip will be calculated by applying the finite element method. Then the stress intensity factors are determined from the results of the reference problem and given unknown problem <sup>(2)</sup> using the same finite element mesh pattern. Here, the most fundamental central interface crack in bonded plate in Fig. 2 will be considered with varying Dundur's parameter  $\alpha, \beta$ . Then, the effects of material combination on the interface stress intensity factors  $K_I, K_{II}$  will be discussed.

## 2. Analysis Method

The analysis method used in this research is based on the stresses at the crack tip calculated by FEM. By using the proportional stress fields for the reference and given problems, stress intensity factors can be obtained with a good accuracy<sup>(5)</sup>. For example, for model I crack in homogenous plates, the stress distribution near the crack tip can be expressed by the following equation.

$$\sigma_y = K_I / \sqrt{2\pi r} \quad (2)$$

It is confirmed that the error of FEM mainly comes from the mesh around the crack tip. Therefore if the same mesh size and pattern are applied to the reference and given unknown problems, stress intensity factors  $K_I$  can be obtained from the stresses  $\sigma_y$  calculated by FEM. At a given distance  $r$ , the following relationship can be derived from Eq.(2).

$$K_I / \sigma_y = const \quad (3)$$

If different crack problems A and B are analyzed by applying the same FEM mesh, the following equation can be given at the same distance from the crack tip.

$$\left[ K_I^* / \sigma_y^* \right]_A = \left[ K_I / \sigma_y \right]_B \quad (4)$$

Here, an asterisk (\*) means the values of the reference problem. By using Eq.4 with stress values at crack tip calculated by FEM, accurate stress intensity factors in homogenous plates were successfully obtained by Nisitani et al<sup>(5),(6)</sup>.

Although this method cannot be applied to interface crack problems without difficulty, an effective method was recently proposed by Oda et al<sup>(2)</sup> successfully to analyze interface crack problems. It is well known that there exists oscillation singularity at the interface crack tip. From the stresses  $\sigma_y, \tau_{xy}$  along the interface crack tip, stress intensity factors are defined as shown in Eq.(5).

$$\sigma_y + i\tau_{xy} = \frac{K_I + iK_{II}}{\sqrt{2\pi r}} \left( \frac{r}{2a} \right)^{i\varepsilon}, \quad r \rightarrow 0, \quad (5)$$

$$\varepsilon = \frac{1}{2\pi} \ln \left[ \left( \frac{\kappa_1 + 1}{G_1 + G_2} \right) / \left( \frac{\kappa_2 + 1}{G_2 + G_1} \right) \right] \quad (6)$$

$$\kappa_j = \frac{3 - \nu_j}{1 + \nu_j} (\text{plane stress}), \kappa_j = 3 - 4\nu_j (\text{plane strain}) \quad (j=1,2)$$

From Eq.(5), the stress intensity factors may be separated as

$$K_I = \lim_{r \rightarrow 0} \sqrt{2\pi r} \sigma_y \left( \cos Q + \frac{\tau_{xy}}{\sigma_y} \sin Q \right), \quad (7)$$

$$K_{II} = \lim_{r \rightarrow 0} \sqrt{2\pi r} \tau_{xy} \left( \cos Q + \frac{\sigma_y}{\tau_{xy}} \sin Q \right), \quad (8)$$

$$Q = \varepsilon \ln \left( \frac{r}{2a} \right). \quad (9)$$

Here,  $r$  and  $Q$  can be chosen as constant values since the reference and unknown problem have the same mesh pattern and material combination. Therefore if Eq.(10) is satisfied, Eq.(11) may be derived from Eq.(10). In such case, oscillatory items of the reference and unknown problems are changed into the same.

$$Q^* = Q, \quad \frac{\tau_{xy}^*}{\sigma_y^*} = \frac{\tau_{xy}}{\sigma_y} \quad (10)$$

$$\frac{K_I^*}{\sigma_y^*} = \frac{K_I}{\sigma_y}, \quad \frac{K_{II}^*}{\tau_{xy}^*} = \frac{K_{II}}{\tau_{xy}} \quad (11)$$

Stress intensity factors of the given unknown problem can be obtained by:

$$K_I = \frac{\sigma_{y0,FEM}^*}{\sigma_{y0,FEM}} K_I^* \quad (12)$$

$$K_{II} = \frac{\tau_{xy0,FEM}^*}{\tau_{xy0,FEM}} K_{II}^* \quad (13)$$

Here,  $\sigma_y^*$ ,  $\tau_{xy}^*$  are stresses of reference problem calculated by FEM, and  $\sigma_y$ ,  $\tau_{xy}$  are stresses of given unknown problem. Stress intensity factors of the reference problem are defined by Eq.(14).

$$K_I^* + iK_{II}^* = (T + iS)\sqrt{\pi a}(1 + 2i\varepsilon) \quad (14)$$

Regarding the reference problem in Fig.4, denote  $\sigma_{y0,FEM}^{T=1,S=0}$ ,  $\tau_{xy0,FEM}^{T=1,S=0}$  are values of stresses for  $(T, S) = (1, 0)$ , and  $\sigma_{y0,FEM}^{T=0,S=1}$ ,  $\tau_{xy0,FEM}^{T=0,S=1}$  are ones for  $(T, S) = (0, 1)$ . In order to satisfy Eq.(10), stresses at the crack tip of the reference problem are expressed as

$$\begin{aligned} \sigma_{y0,FEM}^* &= \sigma_{y0,FEM}^{T=1,S=0} * T + \sigma_{y0,FEM}^{T=0,S=1} * S, \\ \tau_{xy0,FEM}^* &= \tau_{xy0,FEM}^{T=1,S=0} * T + \tau_{xy0,FEM}^{T=0,S=1} * S \end{aligned} \quad (15)$$

By substituting Eq.(10) into Eq.(15) with T=1, the value of S is obtained as

$$S = \frac{\sigma_{y0,FEM} * \tau_{xy0,FEM}^{T=1,S=0} * - \tau_{xy0,FEM} * \sigma_{y0,FEM}^{T=1,S=0} *}{\tau_{xy0,FEM} * \sigma_{y0,FEM}^{T=0,S=1} * - \sigma_{y0,FEM} * \tau_{xy0,FEM}^{T=0,S=1} *} \quad (16)$$

### 3. Stress Intensity Factors of an Interface Crack in a Bonded Infinite Plate

To express the results the following dimensionless stress intensity factors  $F_I, F_{II}$  are used.

$$K_I + iK_{II} = (F_I + iF_{II})(1 + 2i\varepsilon)\sigma\sqrt{\pi a} \quad (17)$$

Dundurs' bi-material parameters  $\alpha, \beta$  are defined in Eq.(18).

$$\alpha = \frac{G_1(\kappa_2 + 1) - G_2(\kappa_1 + 1)}{G_1(\kappa_2 + 1) + G_2(\kappa_1 + 1)}, \quad \beta = \frac{G_1(\kappa_2 - 1) - G_2(\kappa_1 - 1)}{G_1(\kappa_2 + 1) + G_2(\kappa_1 + 1)} \quad (18)$$

#### 3.1 Effect of Plate Dimensions on the Stress Intensity Factors

In order to discuss bonded infinite plates, it is necessary to consider the effect of the plate dimensions on the stress intensity factors because the finite element method cannot treat the infinite plates directly. The results of central interface crack in Fig.2 (a) are therefore investigated in Table 2 with varying  $a/W = 1/1620, 1/3240, 1/6480$  and  $\alpha = 0.75, \beta = 0, \alpha = 0.9, \beta = 0, \alpha = 0.75, \beta = 0.2$ . It is seen that results of  $a/W < 1/1620$  coincide each other and may have more than 3 digit accuracy. In other words, Table 2 shows that the results for  $a/W = 1/1620$  can be used as the infinite plate  $a/W \rightarrow 0$  with less than 0.09% error. It is also seen that  $F_{II} \rightarrow 0$  as  $a/W \rightarrow 0$  under arbitrary material combination. In the following sections, the results for the bonded infinite plate obtained as shown in Table 1 will be discussed.

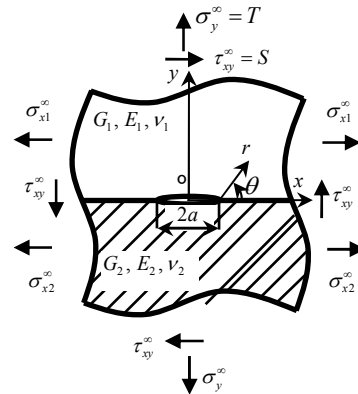


Fig.4 Reference problem ( $\varepsilon_{x1} = \varepsilon_{x2}$  at  $y = 0$ )

**3.2 Central Interface Crack in a Bonded Infinite Plate under Uni-Axial Tension**

Figure 5 shows the results of a central interface crack in a bonded infinite plate under uni-axial tension in the y-direction as shown in Fig.2 (a). In Fig.5, Dundur’s parameter  $\beta$  is fixed, and the variations of  $F_I$  are depicted with varying parameter  $\alpha$ . When material 1 and material 2 are exchanged, Dundur’s parameters  $(\alpha, \beta)$  become  $(-\alpha, -\beta)$ . Then the stress intensity factors  $(F_I, F_{II})$  become  $(F_I, -F_{II})$ . Therefore all material combinations are considered in the range  $\alpha > 0$  in Fig.6( a).

In Fig.5, the solid curves show the results of a central interface crack under remote tension  $\sigma_y = \sigma$ . The dashed lines are extended from solid lines because some cases of material combination are difficult to be obtained by the FEM. The dashed line shows the results of that under internal pressure  $\sigma$  whose solution is known as  $F_I = 1$  and  $F_{II} = 0$ . Figure 5 shows the variation of  $F_I = 0.882 \sim 1.036$ , which has the minimum value  $F_I = 0.882$  when  $\alpha = 1.0, \beta = 0$ , and the maximum value  $F_I = 1.036$  when  $\alpha = 0.2, \beta = 0.3$ . It is also found that  $F_{II} = 0$  for the full range of  $\alpha, \beta$ . Therefore it may be concluded that central interface crack in a bonded infinite plate under remote tension of  $\sigma = 1$  is equivalent to that under internal pressure of  $\sigma = 0.882 \sim 1.036$ . All the values in Fig.5 are given in Table 3 with 3 decimal. From Fig.5 and Table 3, we can conclude that  $F_I > 1.0$  when  $(\alpha + 2\beta)(\alpha - 2\beta) < 0$ ,  $F_I = 1.0$  when  $(\alpha + 2\beta)(\alpha - 2\beta) = 0$  and  $F_I < 1$  when  $(\alpha + 2\beta)(\alpha - 2\beta) > 0$ . In Table 3, values for  $F_I = 1.0$  are marked by underlines.

Table 2 Dimensionless stress intensity factors of crack in Fig.2 (a) with different  $a/W$ .

	$a/W$	$\alpha = 0.75$ $\beta = 0$	$\alpha = 0.75$ $\beta = 0$	$\alpha = 0.75$ $\beta = 0$
$F_I$	1/1620	0.93955	0.90859	0.95516
	1/3240	0.93962	0.90883	0.95515
	1/6480	0.93982	0.90943	0.95514
	$\rightarrow 0$	0.94002	0.91003	0.95513
$F_{II}$	1/1620	$2.21 \times 10^{-4}$	$2.59 \times 10^{-4}$	$1.11 \times 10^{-4}$
	1/3240	$1.10 \times 10^{-4}$	$1.28 \times 10^{-4}$	$5.53 \times 10^{-5}$
	1/6480	$5.51 \times 10^{-5}$	$6.42 \times 10^{-5}$	$2.76 \times 10^{-5}$
	$\rightarrow 0$	0	0	0



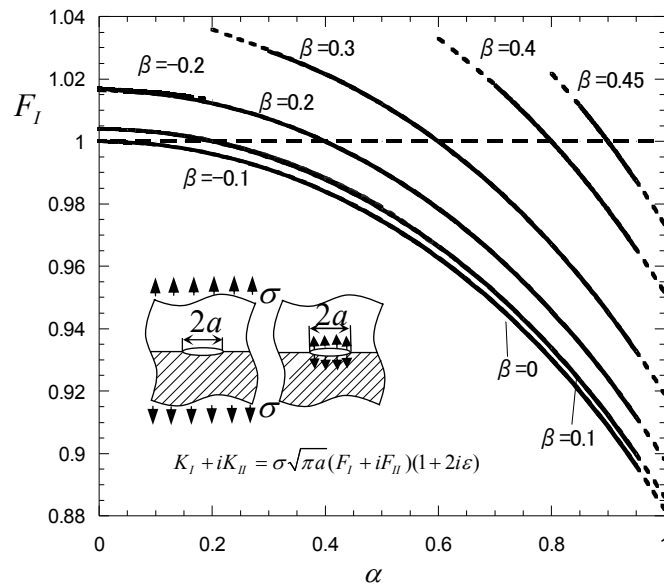
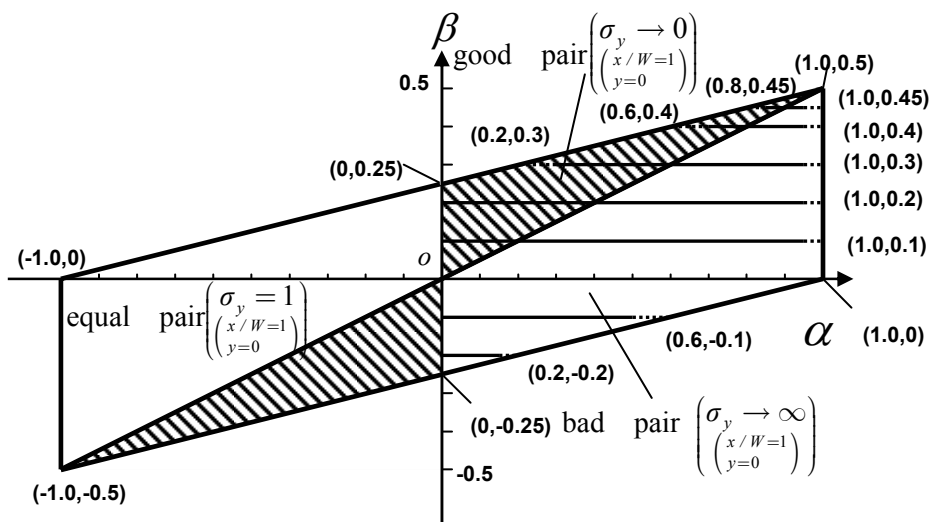


Fig.5  $F_I$  of a central interface crack in a bonded infinite plate under uni-axial tension which is corresponding to Fig.2 (a) with  $a/W \rightarrow 0$ .

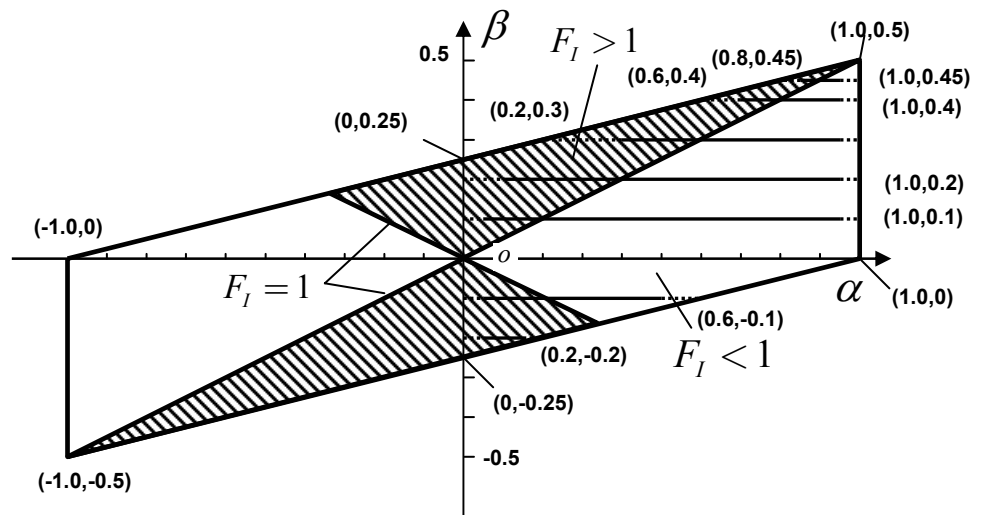
Table 3 Dimensionless stress intensity factor  $F_I$  in Fig.2 (a) with  $a/W \rightarrow 0$ .

— indicates  $F_I = 1$  for  $(\alpha + 2\beta)(\alpha - 2\beta) = 0$  ;  $F_I > 1$  for  $(\alpha + 2\beta)(\alpha - 2\beta) < 0$ ;  $F_I < 1$  for  $(\alpha + 2\beta)(\alpha - 2\beta) > 0$

$\alpha \backslash \beta$	-0.2	-0.1	0	0.1	0.2	0.3	0.4	0.45
0.00	1.017	1.004	1.000	1.004	1.017	—	—	—
0.05	1.016	1.004	1.000	1.004	1.016	—	—	—
0.10	1.016	1.003	0.999	1.003	1.015	—	—	—
0.15	1.015	1.002	0.998	1.002	1.014	—	—	—
0.20	(1.013)	1.000	0.996	1.000	1.012	(1.036)	—	—
0.30	—	0.995	0.991	0.995	1.007	1.029	—	—
0.40	—	0.988	0.984	0.988	1.000	1.022	—	—
0.50	—	0.979	0.975	0.978	0.990	1.012	—	—
0.60	—	(0.966)	0.963	0.966	0.979	1.000	(1.033)	—
0.70	—	—	0.948	0.952	0.964	0.985	1.018	—
0.75	—	—	0.940	0.943	0.955	0.977	1.010	—
0.80	—	—	0.930	0.934	0.946	0.967	1.000	(1.022)
0.85	—	—	0.920	0.924	0.935	0.957	0.990	1.011
0.90	—	—	0.910	0.912	0.924	0.945	0.978	1.000
0.95	—	—	0.896	0.900	0.912	0.933	0.965	0.987
1.00	—	—	(0.882)	(0.886)	(0.898)	(0.919)	(0.952)	(0.974)



(a) Shadow regions  $\alpha(\alpha - 2\beta) < 0$  have no stress singular at the edge  $x = \pm W$  in Fig.2 (a)



(b) Shadow regions  $(\alpha + 2\beta)(\alpha - 2\beta) < 0$  have  $F_I > 1$  for Fig.1 (a) with  $a/W \rightarrow 0$

Fig.6 The map of  $\alpha$  and  $\beta$

### 3.3 Stress Distributions in a Bonded Plate without Crack

Figure 7 shows a bi-material bonded plate without crack under remote tension, which is used to explain the reason why stress intensity factor  $F_I \neq 1$  for the central interface crack. Here, stress distributions at cross-sections a, b, c, d, e in Fig. 7 are investigated under different material combinations.

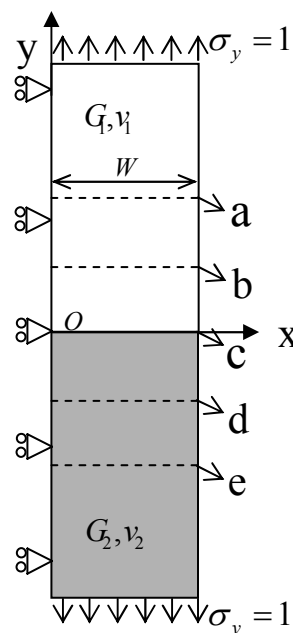


Fig.7 The finite element model in Fig.2 (a) with  $a/W \rightarrow 0$

Figure 8 (a), (b), (c), (d), (e) show the stress distributions for (a)  $\alpha = 0.4, \beta = 0.3$ , (b)  $\alpha = 0.6, \beta = 0.3$ , (c)  $\alpha = 0.7, \beta = 0.1$ , (d)  $\alpha = 0.1, \beta = -0.2$ , (e)  $\alpha = 0.2, \beta = -0.1$  respectively. As can be seen from Fig.8, stresses at cross-sections a, b, c, d, e in Fig.7 are not unity, however, the average stress at each cross-section is equivalent to the remote tension  $\sigma_y = 1$ .

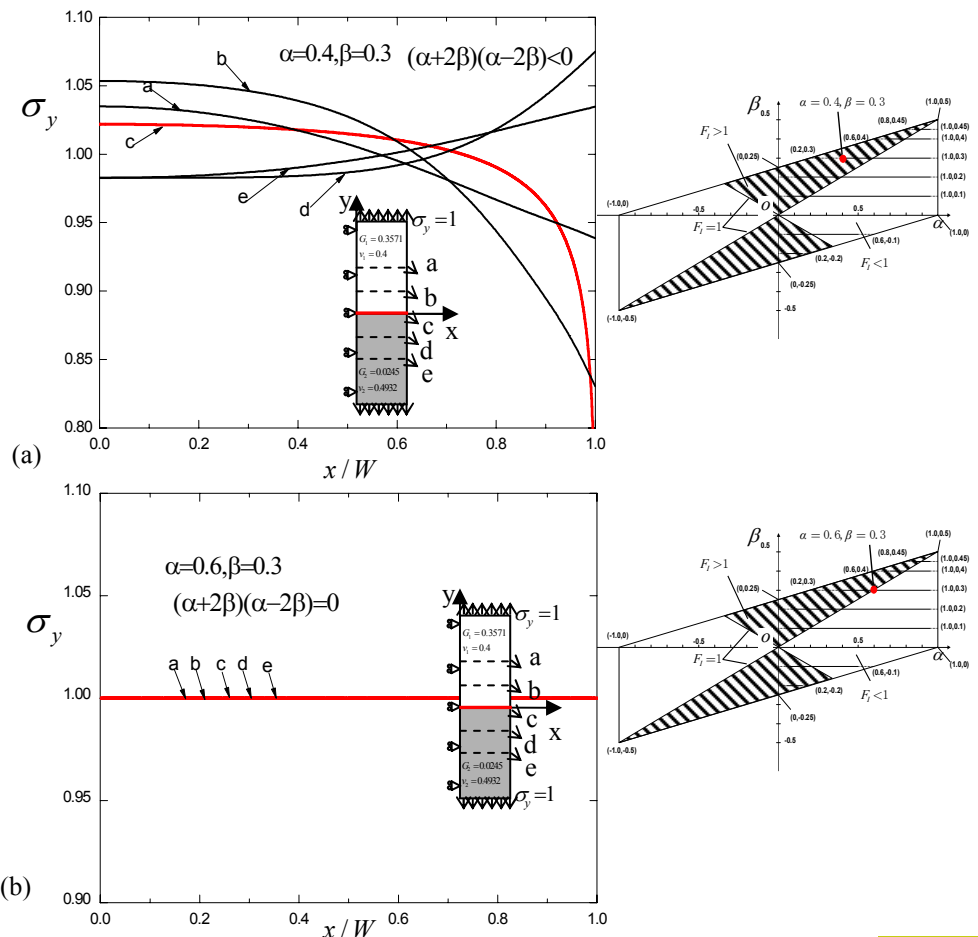
Specifically,  $\alpha = 0.4, \beta = 0.3$  is considered as a good pair since  $\alpha(\alpha - 2\beta) < 0$  is

satisfied as shown in Fig.6 (a). In this case, it is seen that  $\sigma_y = 0$  at the free edge of the interface  $x/W = 1$ . Therefore,  $\sigma_y$  around  $x = 0$  should be larger than 1 which leads to  $F_I > 1$  when  $\alpha(\alpha - 2\beta) < 0$  <sup>(7),(8)</sup>. On the other hand, from Fig.8 (b), constant stress distributions of  $\sigma_y = 1$  at each cross-section are confirmed. Here,  $\alpha = 0.6, \beta = 0.3$  is supposed to be the equal pair since  $\alpha(\alpha - 2\beta) = 0$  as shown in Fig.6 (a). As a result,  $F_I = 1$  appears when  $\alpha(\alpha - 2\beta) = 0$ . Similarly,  $\alpha = 0.7, \beta = 0.1$  satisfies  $\alpha(\alpha - 2\beta) > 0$ , which is regarded as a bad pair as shown in Fig.6 (a). In this case, the stress  $\sigma_y$  at the free interface edge  $x/W = 1$  goes to infinity as  $\sigma_y \rightarrow \infty$ . The stress distributions near  $x = 0$  are therefore should be less than unity as  $\sigma_y < 1$ . This is the reason why  $F_I < 1$  when  $\alpha(\alpha - 2\beta) > 0$ .

Fig.8 (d) indicates stress distributions for  $\alpha = 0.2, \beta = -0.1$  which satisfies bad pair condition  $\alpha(\alpha - 2\beta) > 0$  as shown in Fig.6 (a), and the stress  $\sigma_y$  at the free interface edge  $x/W = 1$  goes to infinity as  $\sigma_y \rightarrow \infty$ , but different from Fig.8 (c), the stress  $\sigma_y$  becomes smaller around  $x/W = 1$ . Then,  $\sigma_y = 1$  appears at  $x = 0$ , which leads to  $F_I = 1$ . Because in this case,  $\alpha$  and  $\beta$  satisfy  $\alpha + 2\beta = 0$ , considering Fig.8 (b) and Fig.8 (d), it can be concluded that  $F_I = 1$  is obtained when  $(\alpha + 2\beta)(\alpha - 2\beta) = 0$ . Figure8 (e) indicates stress distributions for  $\alpha = 0.1, \beta = -0.2$ , similar with Fig.8 (d), although bad pair condition  $\alpha(\alpha - 2\beta) > 0$  is satisfied,  $\sigma_y > 1$  appears at  $x = 0$ , which leads to  $F_I > 1$ . Because in this case,  $\alpha$  and  $\beta$  satisfy  $\alpha + 2\beta < 0$ , considering Fig.8 (a) and Fig.8 (e), it can be conclude that  $F_I > 1$  is obtained when  $(\alpha + 2\beta)(\alpha - 2\beta) < 0$ .

Therefore, there are two lines to control  $F_I$  as shown in Fig.6 (b), one is  $\alpha - 2\beta = 0$  and the other is  $\alpha + 2\beta = 0$ . For  $(\alpha + 2\beta)(\alpha - 2\beta) > 0$ ,  $F_I < 1$ ; for  $(\alpha + 2\beta)(\alpha - 2\beta) = 0$ ,  $F_I = 1$ ; for  $(\alpha + 2\beta)(\alpha - 2\beta) < 0$ ,  $F_I > 1$ .

Table 4 shows the stress at O in Fig.7 comparing with  $F_I$  of a central crack in a bonded infinite plate with varying material combination. From this table, it is found that the stress intensity factor  $F_I$  is equal to the stress  $\sigma_y$  at O in the bonded plate without crack. This leads us to the conclusion that  $F_I$  of an interface crack in a bonded infinite plate can be easily obtained from the stress  $\sigma_y$  at the interface without crack.





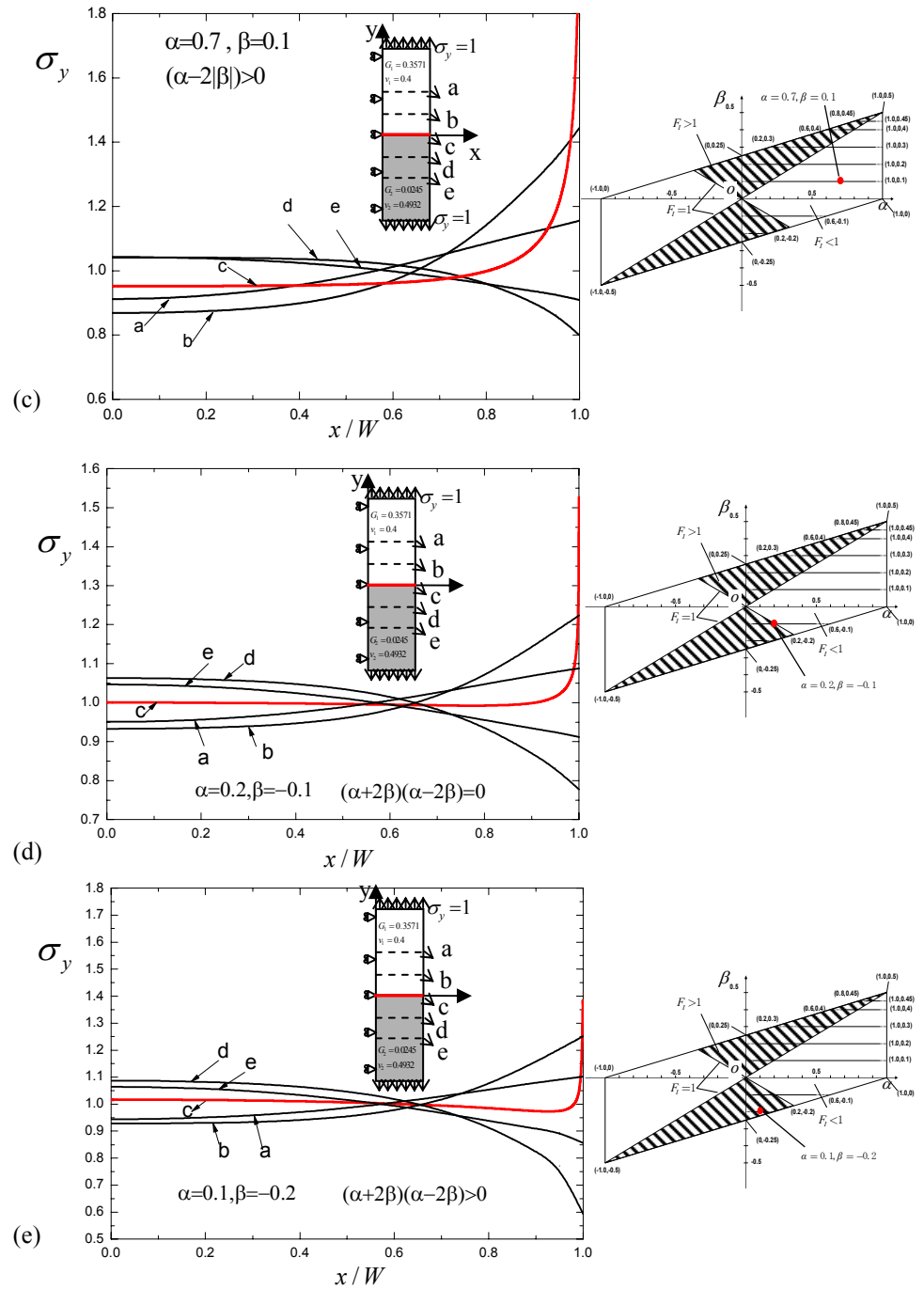


Fig.8 stress distribution  $\sigma_y$  (a)  $\alpha=0.4, \beta=0.3$ , (b)  $\alpha=0.6, \beta=0.3$ , (c)  $\alpha=0.7, \beta=0.1$ , (d)  $\alpha=0.2, \beta=-0.1$ , (e)  $\alpha=0.1, \beta=-0.2$

Table 4 The comparison between  $\sigma_y$  at  $x=0, y=0$  in Fig.7 and  $F_I$  in Fig.2 (a) with  $a/W \rightarrow 0$ .

$\alpha$	$\beta$	$\sigma_y$ at $O$ in Fig.7	$F_I$
0.20	0.0	0.995943	0.995944
0.85	0.0	0.908100	0.908081
0.40	0.3	1.021600	1.021750
0.80	0.4	1.000000	1.000000

**3.4 Central Interface Crack in a Bonded Infinite Plate with Material 1 under Tension in the x-direction**

Table 5 shows stress intensity factors of central interface crack shown in Fig.2(b) with different relative crack size  $a/W = 1/1620, 1/3240, 1/6480$  under different material combination  $\alpha = 0.3, \beta = 0.2, \alpha = -0.75, \beta = 0, \alpha = -0.8, \beta = -0.4$ . It is seen that all the results coincide each other more than 3 digit when  $a/W < 1/1620$ .

Figure 9 shows the results of bonded infinite plate  $a/W \rightarrow 0$  with material 1 under tension in the x-direction. The dashed lines are extended from solid lines because some cases of material combination are difficult to be obtained by the FEM. In Fig.9,  $\beta$  in each curve is fixed, and the variations of  $F_I$  are depicted with varying parameter  $\alpha$ . Previously, it has been thought that tension in the x direction does not contribute to the stress intensity factors<sup>(1)</sup>. However, as can be seen from Fig.9,  $F_I$  is not 0 in current research. It should be noted that the stress intensity factor  $F_I$  is not zero under x-directional tension, except the case when  $\varepsilon_{x1} = \varepsilon_{x2}$  is produced along the interface, and it has the minimum value  $F_I = -0.034$  when  $\alpha = 0.2, \beta = 0.3$ , and the maximum value  $F_I = 0.267$  when  $\alpha = -1.0, \beta = -0.45$ . It is also found that  $F_{II} = 0$  for the central interface crack under x-directional tension. Therefore, it may be concluded that central interface crack in a bonded infinite plate with material 1 under x-directional remote tension is equivalent to that of under internal pressure of  $\sigma = -0.034 \sim 0.267$ . All the values in Fig.9 are provided in Table 6.

**4. Central Interface Crack in a Bonded Finite Plate**

Until here the stress intensity factors of interface crack in bonded infinite plate are mainly treated. In this chapter, the bonded finite plate as shown in Fig.2 (a) is newly

Table 5 Dimensionless stress intensity factors of crack in Fig.2 (b) with different  $a/W$ .

	$a/W$	$\alpha = 0.3,$ $\beta = 0.2$	$\alpha = -0.75,$ $\beta = 0$	$\alpha = -0.8,$ $\beta = -0.4$
$F_I$	1/1620	-0.02540	0.07051	0.17962
	1/3240	-0.02539	0.07056	0.17960
	1/6480	-0.02539	0.07055	0.17959
	$\rightarrow 0$	-0.02539	0.07054	0.17958
$F_{II}$	1/1620	$1.11 \times 10^{-4}$	$2.59 \times 10^{-4}$	$3.28 \times 10^{-4}$
	1/3240	$5.53 \times 10^{-5}$	$1.29 \times 10^{-4}$	$1.64 \times 10^{-4}$
	1/6480	$2.77 \times 10^{-5}$	$6.46 \times 10^{-5}$	$8.19 \times 10^{-5}$
	$\rightarrow 0$	0	0	0

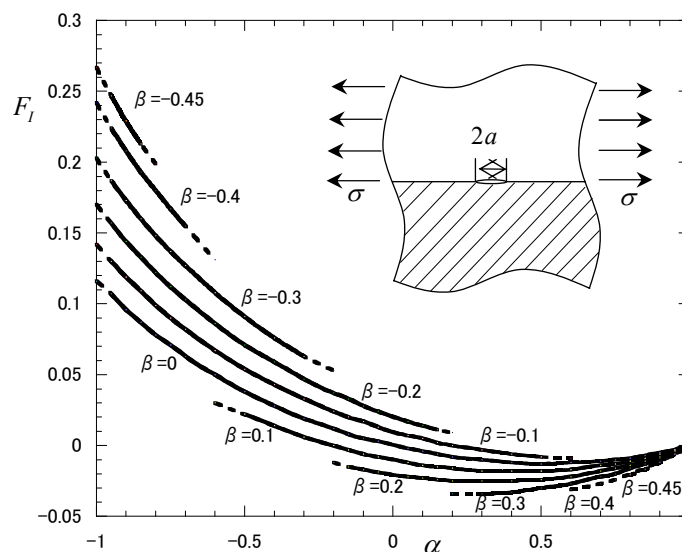


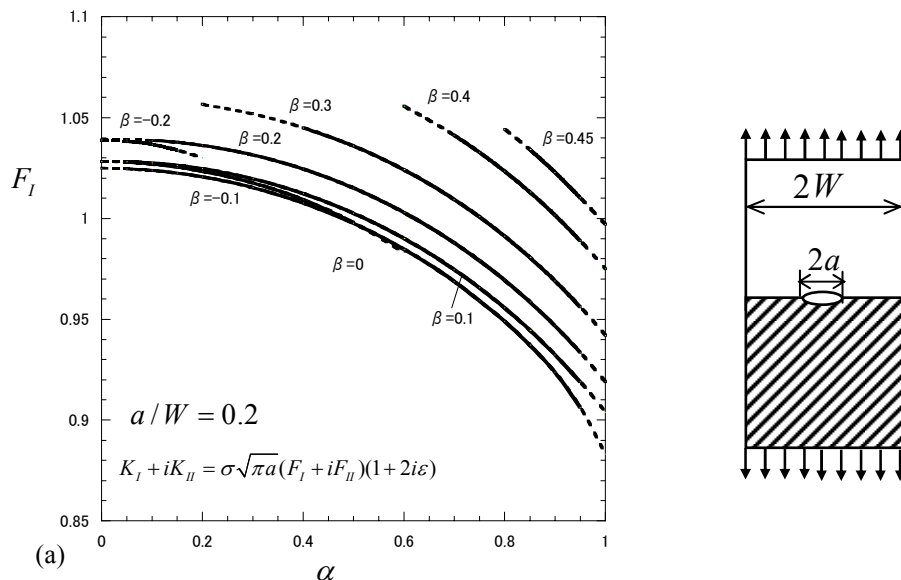
Fig.9  $F_I$  of a central interface crack in a bonded infinite plate under  $\sigma_{x1}^\infty = \sigma$  (see Fig. 2 (b) with  $a/W \rightarrow 0$  )

Table 6 Dimensionless stress intensity factor  $F_I$  in Fig.2 (b) with  $a/W \rightarrow 0$ .

$\alpha \backslash \beta$	-0.45	-0.4	-0.3	-0.2	-0.1	0	0.1	0.2	0.3	0.4	0.45
-1.00	(0.267)	(0.242)	(0.203)	(0.170)	(0.142)	(0.116)	—	—	—	—	—
-0.95	0.247	0.224	0.187	0.157	0.130	0.107	—	—	—	—	—
-0.90	0.229	0.208	0.173	0.144	0.119	0.096	—	—	—	—	—
-0.85	0.213	0.193	0.160	0.133	0.109	0.087	—	—	—	—	—
-0.80	(0.199)	0.180	0.148	0.122	0.099	0.078	—	—	—	—	—
-0.75	—	0.167	0.137	0.112	0.090	0.071	—	—	—	—	—
-0.70	—	0.155	0.127	0.103	0.082	0.063	—	—	—	—	—
-0.60	—	(0.131)	0.108	0.086	0.067	0.050	(0.030)	—	—	—	—
-0.50	—	—	0.091	0.071	0.054	0.038	0.022	—	—	—	—
-0.40	—	—	0.076	0.059	0.043	0.028	0.014	—	—	—	—
-0.30	—	—	0.063	0.047	0.033	0.019	0.006	—	—	—	—
-0.20	—	—	(0.053)	0.037	0.024	0.012	0.000	(-0.012)	—	—	—
-0.15	—	—	—	0.033	0.020	0.008	-0.003	-0.015	—	—	—
-0.10	—	—	—	0.028	0.017	0.005	-0.006	-0.017	—	—	—
-0.05	—	—	—	0.024	0.013	0.003	-0.008	-0.019	—	—	—
0.05	—	—	—	0.017	0.007	-0.002	-0.012	-0.022	—	—	—
0.10	—	—	—	0.014	0.005	-0.004	-0.014	-0.023	—	—	—
0.15	—	—	—	0.011	0.002	-0.006	-0.015	-0.024	—	—	—
0.20	—	—	—	(0.009)	0.000	-0.008	-0.016	-0.025	(-0.034)	—	—
0.30	—	—	—	—	-0.003	-0.010	-0.018	-0.025	-0.034	—	—
0.40	—	—	—	—	-0.006	-0.012	-0.018	-0.025	-0.033	—	—
0.50	—	—	—	—	-0.008	-0.013	-0.018	-0.024	-0.030	—	—
0.60	—	—	—	—	(-0.009)	-0.012	-0.017	-0.022	-0.027	(-0.031)	—
0.70	—	—	—	—	—	-0.011	-0.014	-0.018	-0.022	-0.027	—
0.75	—	—	—	—	—	-0.010	-0.013	-0.016	-0.020	-0.024	—
0.80	—	—	—	—	—	-0.009	-0.011	-0.014	-0.016	-0.020	(-0.021)
0.85	—	—	—	—	—	-0.007	-0.009	-0.011	-0.013	-0.016	-0.017
0.90	—	—	—	—	—	-0.005	-0.006	-0.008	-0.009	-0.011	-0.012
0.95	—	—	—	—	—	-0.003	-0.003	-0.004	-0.004	-0.006	-0.006
1.00	—	—	—	—	—	(-0.002)	(0.001)	(0.001)	(0.001)	(-0.001)	(0.001)

considered. Figures 10 and 11 show the stress intensity factors for  $a/W = 0.2$  and  $a/W = 0.5$ . The dashed lines are extended from solid lines because some cases of material combination are difficult to be obtained by the FEM. Comparing Figs.10, 11 with Fig.5, it is found that the results in Figs.10, 11 have similar variation trends although values in Figs.10, 11 are slightly larger than those of Fig.5. Similar examinations are performed for  $a/W = 0.1-0.9$  in this study.

The maximum and minimum values of  $F_I, F_{II}$  for each  $a/W$  are shown in Table 7 and Fig.12 with varying  $a/W$ . The dashed lines are extended from solid lines because some cases of material combination are difficult to be obtained by the FEM. Here  $F_{I_{homo}}$  is the results of a central crack in a homogeneous plate, and the present results  $F_{I_{homo}}$  coincide with Isida's results <sup>(9)</sup>. In Fig.12 the results are indicated as the ratios of  $F_{I_{max}} / F_{I_{homo}}$  and  $F_{I_{min}} / F_{I_{homo}}$ . It is seen that  $F_{I_{homo}}$  gives almost largest values of  $F_I$ , and the difference between  $F_{I_{max}}$  and  $F_{I_{homo}}$  is less than 4%. On the other hand, the difference between  $F_{I_{min}}$  and  $F_{I_{homo}}$  increases with increasing  $a/W$ . Figure 12(b) shows maximum and minimum absolute values of  $F_{II}$  increases with increasing  $a/W$ . Specifically, the results for  $G_2 / G_1 = 4$  and  $G_2 / G_1 = 100$  in the previous studies <sup>(2)-(4)</sup> are plotted in Fig.12.



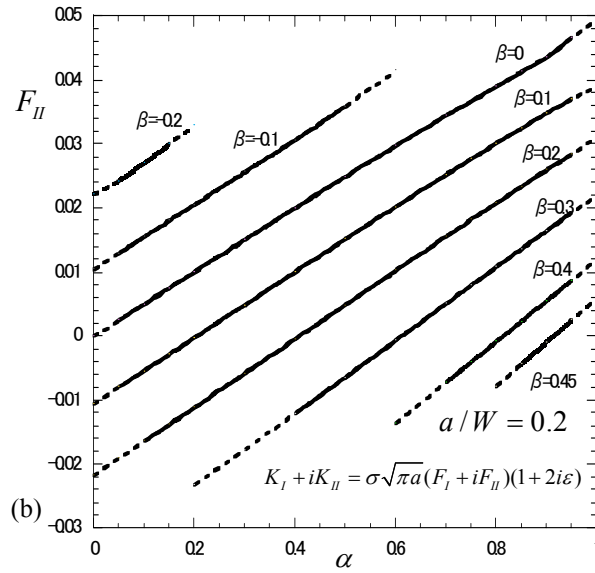


Fig.10 Dimensionless stress intensity factor (a)  $F_I$ , (b)  $F_{II}$  for  $a/W = 0.2$

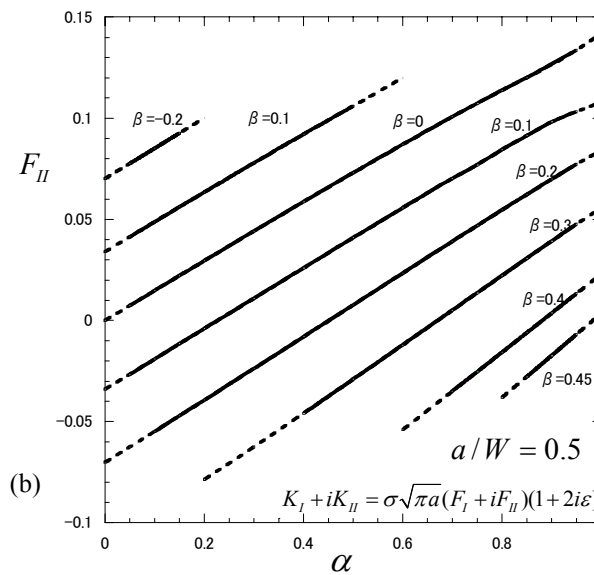
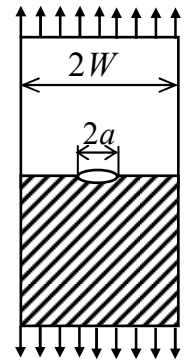
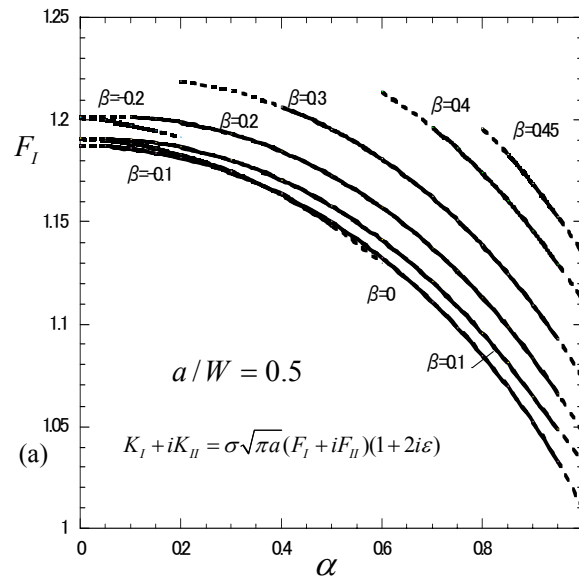


Fig.11 Dimensionless stress intensity factor (a)  $F_I$ , (b)  $F_{II}$  for  $a/W = 0.5$

Table 7 Maximum and minimum values of stress intensity factors  $F_I$ ,  $F_{II}$

$a/W$	$F_{I,max}$	$F_{I,min}$	$F_{I,homo}$	Ref. $F_I$ [9] (homogeneous)	$F_{II,max}$	$F_{II,min}$
→0	1.036	0.882	1.000	1.0000	0	0
0.1	1.039	0.848	1.006	1.0060	0.025	-0.011
0.2	1.057	0.883	1.025	1.0246	0.050	-0.023
0.3	1.089	0.916	1.058	1.0577	0.075	-0.037
0.4	1.141	0.959	1.110	1.1094	0.105	-0.056
0.5	1.219	1.010	1.187	1.1867	0.142	-0.079
0.6	1.336	1.091	1.304	1.3033	0.181	-0.113
0.7	1.519	1.218	1.488	1.4882	0.242	-0.168
0.8	1.842	1.432	1.815	1.8160	0.340	-0.272
0.9	2.582	1.936	2.574	2.5776	0.570	-0.545

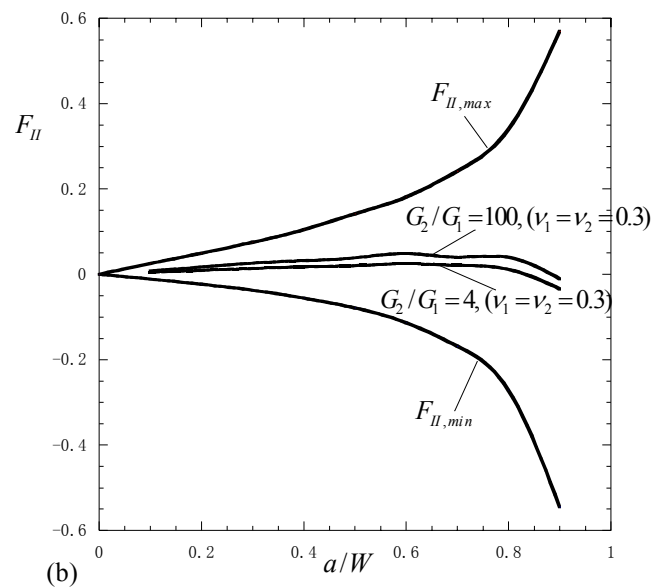
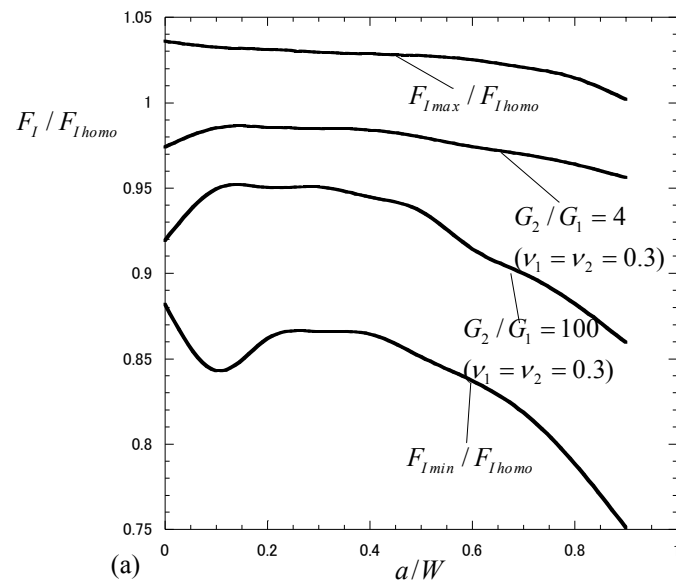
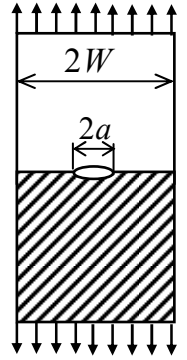


Fig. 12 (a)  $F_{I,max}/F_{I,homo}$ ,  $F_{I,min}/F_{I,homo}$  vs.  $a/W$  and (b)  $F_{II,max}$ ,  $F_{II,min}$  vs.  $a/W$   
( $F_{I,homo}$ : Stress intensity factor for homogeneous plate)



## 5. Conclusions

In this study, stresses at the interface crack tip are calculated by applying the finite element method. Then the stress intensity factors are determined from the results of the reference problem and given unknown problem. The conclusions are given as following.

1. Stress intensity factors of a central interface crack in bonded infinite plate under remote tension were calculated very accurately under arbitrary material combination.
2. Central interface crack in bonded infinite plate under remote tension of  $\sigma = 1$  is equivalent to that under internal pressure of  $\sigma = 0.882 \sim 1.036$ . Moreover, central interface crack in bonded infinite plate with material 1 under remote x-directional tension of  $\sigma = 1$  is equivalent to that under internal pressure of  $\sigma = -0.034 \sim 0.267$ .
3. Variations of the maximum and minimum stress intensity factors  $F_I, F_{II}$  in bonded finite plate are also investigated with varying  $a/W$  in this paper. It is seen that the stress intensity factor for homogeneous material  $F_{I_{homo}}$  gives the maximum value  $F_{I_{max}}$  within 4% error. On the other hand, the difference between  $F_{I_{min}}$  and  $F_{I_{homo}}$  increases with increasing  $a/W$ .

## References

- (1) Yuki, Y., *Mechanics of Interface*, (1992), p. 102, Baifuukan.
- (2) Oda, K., Kamisugi, K., and Noda, N.A., Stress intensity factor analysis of interface cracks based on proportional method, *Transactions of the Japan Society of Mechanical Engineers*, Series A, Vol. 75, (2009), pp. 467-482.
- (3) Matsumoto, T., Tanaka, M. and Obara, R., Stress intensity factor analysis of bimaterial interface cracks based on interaction energy release rate and boundary element sensitivity analysis, *Transactions of the Japan Society of Mechanical Engineers*, Series A, Vol. 65, No. 638 (1999), pp. 2121-2127.
- (4) Miyazaki, N., Ikeda, T., Soda, T., and Munakata, T., Stress intensity factor analysis of interface crack using boundary element method, *Transactions of the Japan Society of Mechanical Engineers*, Series A, Vol. 57, No. 541 (1991), pp. 2063-2069.
- (5) Teranisi, T., and Nisitani, H., Determination of highly accurate values of stress intensity factor in a plate of arbitrary form by FEM, *Transactions of the Japan Society of Mechanical Engineers*, Series A, Vol. 65, (1999), pp. 16-21.
- (6) Nisitani, H., Teranisi, T., and Fukuyama, K., Stress intensity factor analysis of a biomaterial plate based on the crack tip stress method, *Transactions of the Japan Society of Mechanical Engineers*, Series A, Vol. 69, (2003), pp. 1203-1208.
- (7) Bogy, D.B., Edge-bonded dissimilar orthogonal elastic wedges under normal and shear loading, *Journal of Applied Mechanics*, Vol. 35, (1968), pp. 460-466.
- (8) Bogy, D.B., Two edge-bonded elastic wedges of different and wedge angles under surface tractions, *Journal of Applied Mechanics*, Vol. 38, (1971), pp. 377-386.
- (9) Isida, M., *Elastic analysis and stress intensity factor of crack*, (1976), p. 145, Baifuukan.